

# Non-destructive determination of chemical effects on fluorescence yields and vacancy transfer probabilities of tin compounds

Ahmet Tursucu<sup>1\*</sup>, Mehmet Haskul<sup>2</sup> and Asaf Tolga Ulgen<sup>3</sup>

<sup>1</sup> Department of Energy Systems Engineering, Faculty of Engineering, Sirtak University, Sirtak 73000, Turkey, ahmettursucu@sirtak.edu.tr

<sup>2</sup> Department of Mechanical Engineering, Faculty of Engineering, Sirtak University, Sirtak 73000, Turkey, mehmethaskul@gmail.com.tr

<sup>3</sup> Department of Electric and Electronic Engineering, Faculty of Engineering, Sirtak University, Sirtak 73000, Turkey, ulgen\_at@sirtak.edu.tr

## ABSTRACT

In the current work, it was investigated to the K X-ray fluorescence efficiency and chemical effect on vacancy transfer probability for some tin compounds. We used Br<sub>2</sub>Tin, TinI<sub>2</sub>, SeTin, TinF<sub>2</sub>, TinSO<sub>4</sub>, TinCl<sub>2</sub>, TinO and TinS compounds for experimental study. The target samples were irradiated with <sup>241</sup>Am annular radioactive source at the intensity of 5 Ci which emits gamma rays at wavelength of 0.2028 nm. The characteristic x-rays emitted because of the excitation are collected by a high-resolution HPGe semiconductor detector. It has been determined that the experimental calculations of the tin (Sn) element are compatible with the theoretical calculation. In addition, we have calculated the experimental intensity ratios, fluorescence yields and total vacancy transfer probabilities for other Sn compounds.

**Keywords:** vacancy transfer probability; intensity ratio; fluorescence efficiency.

## 1. Introduction

The characteristic X-rays are an electromagnetic wave type that is produced by passing the dissociating electron of an inner layer electron from a high-energy level to a low-energy level<sup>[1]</sup>. When a monochromatic X-ray diffraction onto the material, the scattered, diffracted, and radiographic absorbed events that are the basis of X-ray diffraction occur. A stimulated atom radiative or non-radiative will transition and these transitions continue until reaching the equilibrium state. Stimulation of the outer orbit of the atom; it's internal orbit electrons are possible with stimuli such as accelerated electrons, neutrons,  $\alpha$ -particles, photons emitted from radioactive sources. Thus, a vacancy is formed in the outer shell of the excited atom, these are filled by radiative or non-radiative transition (Auger)<sup>[2]</sup>. The vacancy transfer is called the vacancy from the bottom layer to the top layer<sup>[3]</sup>. Absorption jump factor and jump ratios are important parameters related to the absorption and emission of x-rays that produce fluorescence effect. In the literature, different experimental methods have been used to calculate K shell absorption leap factor and jump ratios, such as gamma ray absorption method<sup>[4-7]</sup>. This method is preferred for the analysis of photons and energy-separated x-ray spectroscopy which are absorbed because of Compton scattering. Absorption jump factor and jump ratio is give ( $K_{\beta}/K_{\alpha}$ ) intensity ratio<sup>[8,9]</sup> and this parameter is also very important in our study. The calculation of the severity rates of the different elements and compounds has several effects on the sample of stimulating radiation and the characteristic properties of the materials used as target specimens are revealed.

The experimental studies of X-ray intensity ratios for different elements are also benefit research areas such as atomic, molecular and radiation physics, geology, medical physics and elemental analysis<sup>[10-12]</sup>. Yılmaz studied the  $K_{\beta}/K_{\alpha}$  intensity ratio at 16.896 keV excitation energy in the elements with atomic numbers between  $28 \leq Z \leq 39$ , using Si (Li) semiconductor detector and compared the calculated experimental values with other theoretical values<sup>[13]</sup>. Baydaş

and Öz worked the chemical effect on  $K_{\beta}$  and  $K_{\beta 1,3}$  publishing lines in some iron compounds using Wavelength Dispersive X-ray Fluorescence (WDXRF) technique and they observed that the oxidation rate of Fe, the main atom in the compounds, is influential in the intensity ratios of the emission lines<sup>[14]</sup>. Porikli *et al* investigated L X-ray intensity ratios and chemical effects on related line structures in some compounds of La, Ce and Pr elements<sup>[15]</sup>. They have proved that, the full width at half maximum (FWHM) values and the spectral lines are susceptible to changes in the molecular structure of the ligand bond.

In this paper, we have studied the chemical effects on the  $K_{\beta}/K_{\alpha}$  x-ray intensity ratio values, K x-ray fluorescence cross sections and K-L shell gap crossing probabilities in Sn compounds. Moreover, in space researches and its compounds which are frequently used as coating materials in industrial devices have been studied. The  $Br_2Sn$ ,  $TiIn_2$ ,  $SeTi$ ,  $TiF_2$ ,  $TiSO_4$ ,  $TiCl_2$ ,  $TiO$  and  $TiS$  samples were also investigated with a high-resolution HPGe semiconductor detector.

## 2. Materials and Methods

In this experimental study, we aimed to calculate the  $K_{\beta}/K_{\alpha}$  x-ray intensity ratio of tin (Sn) compounds using gamma rays of 0.2082 nm wavelength emitted from a 241 Am annular (ring) source at 5 Ci power. The characteristic x-rays which are generated because of gamma rays warping the target sample were collected by a high-resolution semiconductor HPGe detector. This detector has a high purity germanium crystal with 16 mm radius, 10 mm long, and 0.12 mm thick Be window and its active area is 200 mm<sup>2</sup>. The schematic diagram of experimental setup is shown in Fig.1 and Fig.2. A bias voltage of -1500 V was applied to the detector with an ideal resolution of 182 eV at 5.9 keV. The mass thicknesses of the Sn compounds used range from 0.244 to 0.538 g/cm<sup>2</sup> and these samples were  $Br_2Sn$ ,  $TiIn_2$ ,  $SeTi$ ,  $TiF_2$ ,  $TiSO_4$ ,  $TiCl_2$ ,  $TiO$  and  $TiS$ . Spectrum of Sn samples was assessed by using a Canberra (AccuSpec) Pc-based multichannel analyzer card. We fixed the time constant of the Ortec model 472 amplifier at 6  $\mu$ s so that we get the best count value from the detector. Operating parameters of the experimental system were controlled by the computer program Genie-2000. The experimental data were obtained on 1024 channels of the MCA. These data were analyzed and illustrated by the Origin 7.5 software program.

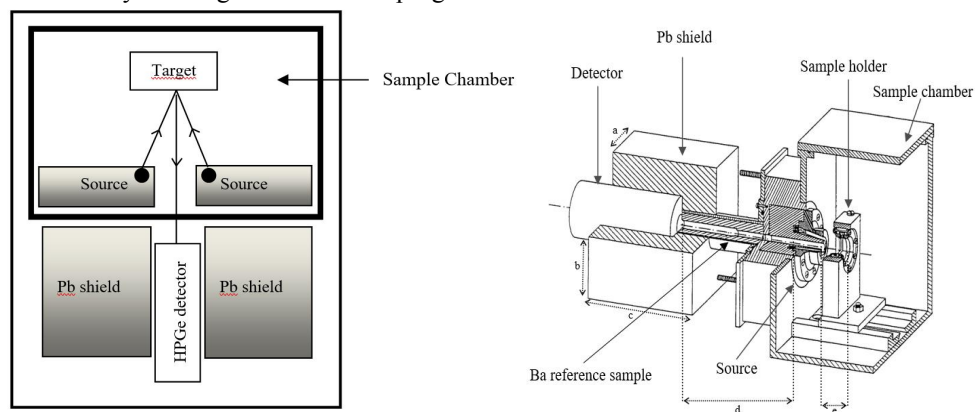


Figure 1. Experimental setup.

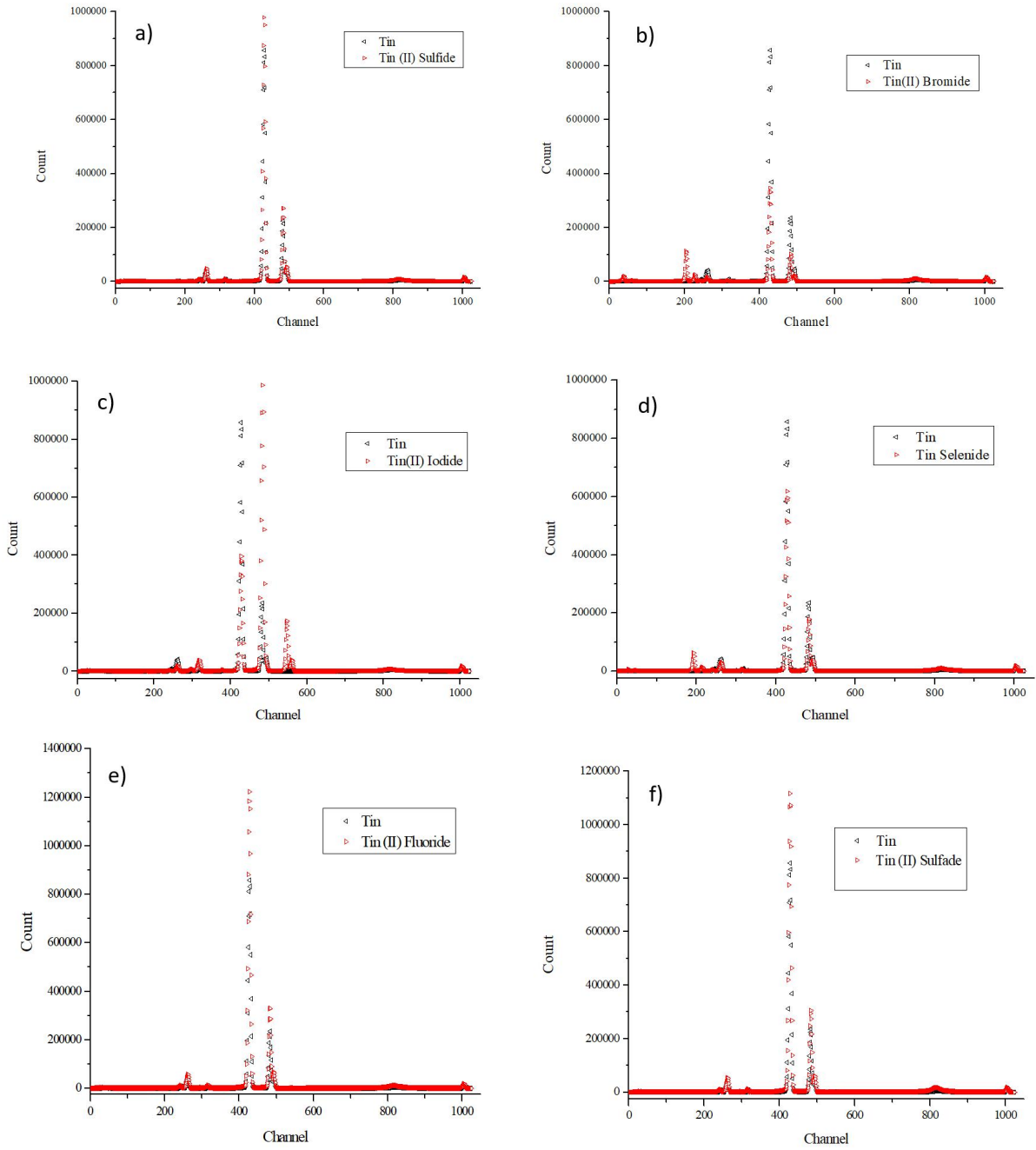


Figure 2. Sample chamber (a=6.5 cm, b=6.3 cm, c=13.5 cm, d=11 cm and e=5 cm).

### 3. Theory

#### 3.1 Calculation of K X-ray Intensity Ratio

The intensity ratios of emitted characteristic K X-rays are the result of filling the vacancy formed by the photoionization of the K layer. Theoretical atomic parameters of K layer are given by the expression

$$I_{K_i} = I_K(E)w_K F_{K_i} \rightarrow i = \alpha, \beta \quad (1)$$

where  $I_K(E)$  is X-ray intensity at excitation energy for element K layer<sup>[16]</sup> and  $w_K$  is the fluorescence efficiency for K layer<sup>[17]</sup>. The  $F_{K_i}$  value is partial emission rate for  $K_i$  X-rays.  $K_{\alpha}$  and  $K_{\beta}$  X-rays are given by the expression

$$F_{K_{\alpha}} = [1 + (I_{K_{\beta}}/I_{K_{\alpha}})]^{-1} \quad \text{and} \quad F_{K_{\beta}} = [1 + (I_{K_{\alpha}}/I_{K_{\beta}})]^{-1}. \quad (2)$$

The  $I_{K_{\beta}}/I_{K_{\alpha}}$  values are taken from the table of Scofield et al. studies[16]. The characteristic of the XRF technique is that the X-ray line intensity is experimentally given as

$$I_{K_i} = N_{K_i}[I_0 G \epsilon_{K_i} \beta t]^{-1} \quad (3)$$

where  $N_{Ki}$  is net peak area in counts,  $I_0$  is severity of stimulated radiation,  $G$  is geometry factor,  $\varepsilon_{K_i}$  is the detector efficiency for  $K$  X-rays group and  $t$  is mass thicknesses of samples ( $\text{g}/\text{cm}^2$ ).  $\beta$  is the self-absorption correction coefficient for incident photons and emitted X-ray photons, as calculated by

As can be seen from Table 1 and Table 2.	Present Exp.	Theoretical	Other Exp.
--	--------------	-------------	------------

$$\beta_{Ki} = \frac{1 - \exp[-(\mu_i/\cos\theta_1 + \mu_e/\cos\theta_2)t]}{(\mu_i/\cos\theta_1 + \mu_e/\cos\theta_2)t} \quad (4)$$

Where  $\mu_i$  and  $\mu_e$  are the mass absorption coefficients of incident and scattered photons, respectively.  $\theta_1$  and  $\theta_2$  are the angles of the excitation photons and the X-rays emitted by the surface normal of the working sample geometry, respectively. In this study,  $\theta_1 = 167.5^\circ$  and  $\theta_2 = 0^\circ$ .  $\mu_i$  and  $\mu_e$  values can be calculated using the WinXCOM[18] software. Equation 4 can also be written as

$$I_0 G \varepsilon_{K_i} = N_{K_\alpha} [I_{K_\alpha} \beta t]^{-1} \quad (5)$$

If the values of  $I_{K_\alpha}$  are used in different excitation energies in Equation 5,  $I_0 G \varepsilon$  can be calculated for any energy. If these values are plotted as a function of the excitation energy  $E$ , the  $I_0 G \varepsilon$  value in the excitation photon energy used in the actual measurements in this graph can be calculated. As a function of  $I_0 G \varepsilon$  energy value;

$$E_{K_\alpha}^3 \log(I_0 G \varepsilon) = A_0 + A_1 \cdot E_{K_\alpha}^1 + A_2 \cdot E_{K_\alpha}^2 + A_3 \cdot E_{K_\alpha}^3 + A_4 \cdot E_{K_\alpha}^4 \quad (6)$$

where  $E_{K_\alpha}$  is energy of  $K_\alpha$  X-rays and  $A_0, A_1, A_2, A_3,$  and  $A_4$  are constants found by the least squares method. Thus, the difference between fitted values and experimental values is less than 2%. Since this difference is not the single energetic peak of the  $K_\beta$  or  $K_\alpha$ , and therefore the average value calculated for energy does not represent energy fully. According to Equation (3) is used for the  $K$  X-ray intensity ratios,

$$\frac{I_{K_\beta}}{I_{K_\alpha}} = \frac{N_{K_\beta}}{N_{K_\alpha}} \frac{\beta_{K_\alpha}}{\beta_{K_\beta}} \frac{\varepsilon_{K_\alpha}}{\varepsilon_{K_\beta}} \quad (7)$$

where  $N_{K_\beta}$  and  $N_{K_\alpha}$  are net counts,  $\beta_{K_\beta}$  and  $\beta_{K_\alpha}$  are the self-absorption correction coefficients, and  $\varepsilon_{K_\alpha}$  and  $\varepsilon_{K_\beta}$  are detector efficiency.

### 3.2 The calculation of K X-ray Fluorescence Yield

For all the selected target samples, the x-ray production cross section at 0.2028 nm wave length excitation energy,

$$\sigma_{K_\alpha} = \sigma_K W_K f_{K_\alpha}$$

as; (8)

where  $w_K$  is fluorescence yield for  $K$  Shell and the theoretical calculation of this value is calculated by Krause worked<sup>[19]</sup>. The  $\sigma_K$  value is the total ionisation cross section of the  $K$  shell, and  $f_{K_\alpha}$  value represents the partial emission ratio. As a result, fluorescence effect cross section, as per the relation;

$$W_K = \frac{\sigma_{K_i}}{\sigma_K} \quad (9)$$

The experimental calculation of clearance transitions ( $\eta_{KL}$ ) from Layer  $K$  to Layer  $L$  is expressed by

$$\eta_{KL} = \frac{2 - w_K}{1 + (I_{K_\beta} + I_{K_\alpha})} \quad (10)$$

## 4. Result and Discussion

In this work, the clearance transitions probabilities ( $\eta_{KL}$ ), intensity ratios and ( $I_{K_\beta}/I_{K_\alpha}$ ) x-ray fluorescence efficiencies ( $W_K$ ) of the  $\text{Sn}$ ,  $\text{Br}_2\text{Sn}$ ,  $\text{SnI}_2$ ,  $\text{SeSn}$ ,  $\text{SnF}_2$ ,  $\text{SnSO}_4$ ,  $\text{SnCl}_2$ ,  $\text{SnO}$  ve  $\text{SnS}$  compounds (from layer  $K$  to layer  $L$ ) were calculated by the above equations. The energy dispersive X-Ray fluorescence spectra of pure  $\text{Sn}$  element and several  $\text{Sn}$  compounds are given in Fig.3.  $K_\beta/K_\alpha$  x-ray intensity ratios,  $K$  x-ray fluorescence yields and  $K$ - $L$  total vacancy transfer probabilities values for the  $\text{Sn}$  sample are given in Table 1. At the same time, experimental values and theoretical values were compared for these sample. Since there is no previous theoretical study for other samples, only experimental values are given as in Table 2.

Intensity Ratios	0,2061	0,22 <sup>a</sup> 0,2061 <sup>b</sup>	0.2086±0.011 <sup>c</sup> 0.226±0.020 <sup>d</sup>
Fluorescence Yields	0.862±0.044	0.862 <sup>a</sup> 0.860 <sup>b</sup>	0.858±0.069 <sup>c</sup> 0.747±0.060 <sup>c</sup>
Vacancy Transfer Probabilities.	0.925±0.0008	0.941 <sup>a</sup> 0.952 <sup>b</sup>	0.942±0.005 <sup>c</sup>

**Table 1.** Values of  $K_{\beta}/K_{\alpha}$  x-ray intensity ratios, K x-ray fluorescence yields and K-L total vacancy transfer probabilities for the Tin sample.

Sample	Intensity Ratios	Fluorescence Yields	Vacancy Transfer Probabilities
TinS	0,2064±0,0003	0,7064 0,1206	1,072 0,1110
Br2Tin	0,2168±0,0107	0,7004 0,1246	1,067 0,1077
TinI2	0,2074±0,0013	0,7058 0,1211	1,072 0,1107
SeTin	0,2465±0,0404	0,6838 0,1349	1,056 0,0981
TinF2	0,2351±0,0289	0,6902 0,1311	1,0605 0,1018
TinSO4	0,2350 ±0,0289	0,6903 0,1309	1,0604 0,1017
TinCl2	0,2343±0,0282	0,6908 0,1306	1,0607 0,1019
TinO	0,2363±0,0302	0,6896±0,1314	1,0598 0,1013

**Table 2.** Experimental values of  $K_{\beta}/K_{\alpha}$  x-ray intensity ratios, K x-ray fluorescence yields and K-L total vacancy transfer probabilities for the other Sn samples.

Sn compounds are found to be effective on x-ray fluorescence parameters of chemical bond structures.

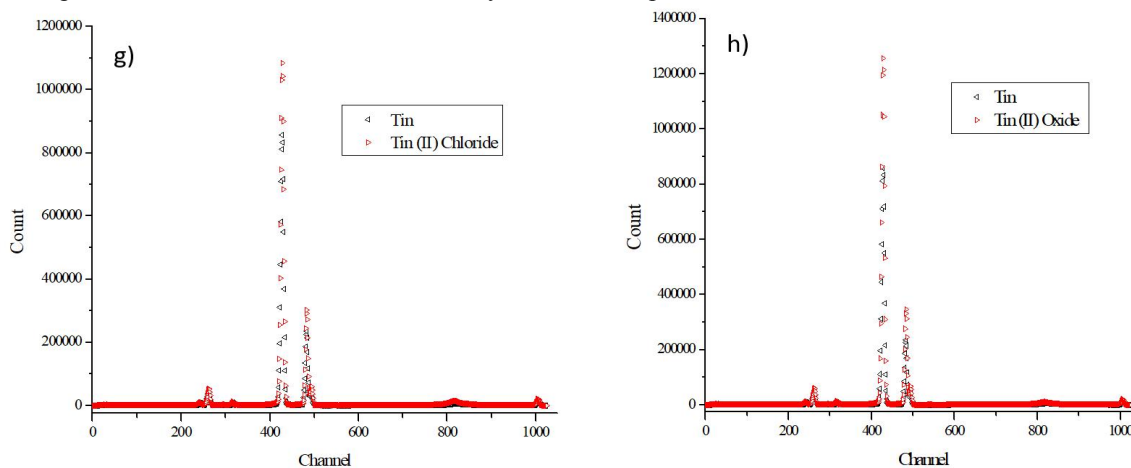


**Figure 3.** Energy Dispersive X-Ray Fluorescence graph for pure Sn (black dots) and Sn compounds (red dots). a) Tin and Tin(II)Sulfide, b) Tin and Tin(II)Bromide, c) Tin and Tin(II)Iodide, d) Tin and TinSelenide, e) Tin and Tin(II)Fluoride, f) Tin and Tin(II)Sulfate, g) Tin and Tin(II)Chloride, f) Tin and Tin(II)Oxide.

The energy dispersive X-Ray fluorescence spectra of pure Sn (black dots) and their compounds (red dots) are depicted in Fig.3. The difference in the characteristic peaks was caused by chemical bond structure and ligand effect, as can be clearly seen from the spectra. As a result, it is seen that some of the peak count numbers are excessive whereas the other peak count numbers are less. This is mainly due to differences in the binding energies of the electrons in the structures connected to the central atom. The differences in the spectrum are based on the common use of the donor electrons made with the main element and the possibility of interacting with the gamma rays in the 0.2082 nm wavelength sent by the density of the exposed electrons.

## 5. Conclusion

The study was observed to be very consistent when compared with theoretical and other experimental data. We have presented the pure Sn element and Sn compounds with scattering intensity ratio, K x-ray fluorescence yields and K-L total vacancy transfer probabilities. Only experimental and theoretical value of the tin element was given in this study and experimental values were calculated for the TinS, Br<sub>2</sub>Tin, TinI<sub>2</sub>, SeTin, TinF<sub>2</sub>, TinSO<sub>4</sub>, TinCl<sub>2</sub> and TinO compounds which will shed light on other theoretical studies. Scattering intensity ratio, K x-ray fluorescence yields and K-L total vacancy transfer probabilities values in all samples are consistent with each other. Additionally, scattering intensity ratio is approximately 0.2, fluorescence yields is ~ 0.7 and total vacancy transfer probabilities values is 1.0 in all samples. It is important to perform similar studies in different excitation energies and detection systems to obtain more detailed and stable results.

## Author Contributions

In the preparation of this manuscript, the first writer contributed 35%, the second writer 30%, the third writer 35%.

## Acknowledgements

This work is supported by Sirmak University Research Fund (BAP), Project no: 2017.03.03.03.

## References

1. Ino S. Theory of transmission coefficient of X-rays evanescent wave for grazing incidence. *Journal of the Physical Society of Japan*.1996; 65(10): 3248-3253.
2. Bieske EJ, Soliva A, Welker MA, *et al*. The B← X electronic spectrum of N<sub>2</sub>+He. *The Journal of Chemical Physics*.1990; 93(6): 4477-4478.
3. Bonzi EV. Measurement of the radiative vacancy transfer probabilities from the L<sub>3</sub> to M and to N shells for W, Re and Pb using synchrotron radiation. *Nuclear Instruments and Methods in Physics Research Section B: Beam Interactions with Materials and Atoms*.2006;245(2): 363-366.
4. Tombesi F, Cappi M, Reeves JN, *et al*. Evidence for ultra-fast outflows in radio-quiet AGNs-I. Detection and statistical incidence of Fe K-shell absorption lines. *Astronomy & Astrophysics*.2010; 521, A57.
5. Bernal AS, Badiger NM (2007). Measurement of K shell absorption and fluorescence parameters for the elements Mo, Ag, Cd, In and Sn using a weak gamma source. *Journal of Physics B: Atomic, Molecular and Optical Physics*.2007; 40(11): 2189.
6. Sidhu BS, Dhaliwal AS, Mann KS, *et al* (2011). Measurement of K-shell absorption edge jump factors and jump ratios of some medium Z elements using EDXRF technique. *Radiation Physics and Chemistry*. 2001; 80(1): 28-32.
7. Oen OS, Holmes DK. Cross sections for atomic displacements in solids by gamma rays. *Journal of Applied Physics*.1959; 30(8): 1289-1295.
8. Budak G, Polat R. Measurement of the K X-ray absorption jump factors and jump ratios of Gd, Dy, Ho and Er by attenuation of a Compton peak. *Journal of Quantitative Spectroscopy and Radiative Transfer*.2004; 88(4): 525-532.
9. Niranjana KM, Krishnananda, Badiger NM, *et al* . Determination of K shell parameters of silver using high resolution HPGe detector spectrometer. *International Journal of Nuclear Energy Science and Technology*.2003; 7(3): 179-190.
10. Han I, Şahin M, Demir L, *et al*. Measurement of K X-ray fluorescence cross-sections, fluorescence yields and intensity ratios for some elements in the atomic range 22 ≤ Z ≤ 68. *Applied radiation and isotopes*. 2007; 65(6): 669-675.
11. Jacob G, Kisch HJ, van der Pluijm. The relationship of phyllosilicate orientation, X-ray diffraction intensity ratios, and c/b fissility ratios in metasedimentary rocks of the Helvetic zone of the Swiss Alps and the Caledonides of Jaemtland, central western Sweden. *Journal of Structural Geology*. 2002; 22(2): 245-258.
12. Ertuğral B, Apaydın G, Çevik U, *et al*; Kβ/Kα X-ray intensity ratios for elements in the range 16 ≤ Z ≤ 92 excited by 5.9, 59.5 and 123.6 keV photons. *Radiation Physics and chemistry*.2007; 76(1): 15-22.
13. Yılmaz R. Kβ/Kα X-ray intensity ratios for some elements in the atomic number range 28 ≤ Z ≤ 39 at 16.896 keV. *Journal of Radiation Research and Applied Sciences*.2017; 10(3):172-177.
14. Baydaş E, Öz E. Chemical effects in the Kα and Kβ<sub>1, 3</sub> of X-ray emission spectra of Fe. *Journal of Electron Spectroscopy and Related Phenomena*.2012; 185(1-2), 27-31.
15. Porikli S. Influence of the chemical environment changes on the line shape and intensity ratio values for La, Ce and Pr L lines spectra. *Chemical Physics Letters*. 2011; 508(1-3), 165-170.
16. Scofield JH. Theoretical photoionization cross sections from 1 to 1500 keV (No. UCRL--51326). California Univ., Livermore. Lawrence Livermore Lab, 1973.
17. Hubbell JH, Trehan PN, Singh N, *et al*. A Review, Bibliography, and Tabulation of K, L, and Higher Atomic Shell

X - Ray Fluorescence Yields. Journal of Physical and Chemical Reference Data.2004; 23(2): 339-364.

18. Gerward L, Guilbert N, Jensen KB, *et al.* (2001). X-ray absorption in matter. Reengineering XCOM. Radiation Physics and Chemistry.2001; 60(1-2):23-24.
19. Krause MO. (1979). Atomic radiative and radiationless yields for K and L shells. Journal of physical and chemical reference data.1979; 8(2): 307-327.